CrossMark

Study of mechanical behavior, deformation, and fracture of nano-multilayer coatings during microindentation and scratch test

**Kaouthar Khlifi, Hafedh Dhiflaoui, Lassaad Zoghlami,
Ahmed Ben Cheikh Larbi**

Abstract Nano-multilayer PVD thin films were deposited on 100C6 (AISI 52100) steel substrate by a PVD magnetron sputtering system. The morphological and microstructural properties were evaluated by using atomic force microscopy and scanning electron microscopy. Residual stresses in all coatings were determined by XRD using the $\sin2\psi$ method. Microindentation and scratch tests were performed, respectively, with a Vickers hardness testing machine and scratch test. These tests were carried out on several coatings with various structures, and compositions TiN single layer, TiAlN multilayer, and TiN/TiAlN nano-multilayer. Hardness measurements were performed by using Vickers imprint using the Jonsson and Hogmark model. Critical loads were measured by scratch test. The results show that the coatings topography was dominated by domes and craters which were uniformly distributed over the surface, and all coatings showed a columnar structure. Damage mechanisms under microindentation and scratch depended on coatings structure and composition. Mechanical and structural properties control the damage behavior and the adhesion quality of coatings. The multilayer structure provides an increase in residual stress, hardness, and failure resistance and a decrease in cracks propagation and adhesion resistance.

K. Khlifi (✉), H. Dhiflaoui, L. Zoghlami,
A. Ben Cheikh Larbi
Ecole Supérieure des Sciences et Techniques de Tunis,
Université de Tunis, 5 Taha Hussein street, 1008 Tunis,
Tunisia
e-mail: khlifi.kaouthar@yahoo.fr

H. Dhiflaoui
e-mail: dhafedh@gmail.com

L. Zoghlami
e-mail: zoghlami-lassaad@hotmail.com

A. Ben Cheikh Larbi
e-mail: ahmed.cheikhlarbi@gmail.com

Introduction

Physical vapor deposited (PVD) coating with a thin film of micron or submicron thickness presented an adequate solution for improving materials' performance in order to satisfy industrial requirements.[1] Several materials have been presented as candidates to produce a thin film by the PVD process. Among this multitude of materials, the titanium nitrides based coatings can be seen as reference coatings because of their high mechanical properties,[2] high temperature resistance, and good tribological behavior.[3] Many situations can be envisioned in industrial applications as we have seen in our previous work.[4] In this latter work, we studied three types of coating such as TiN single layer, TiAlN multilayer. and TiN/TiAlN nano-multilayer that belong to this family of titanium based coating. The objective for studying three types of coatings that belong to the same type of family of titanium coating is to identify the contribution of this new generation of nano-multilayer thin film, and also to prove the improvement of mechanical properties when moving from a TiN single layer to a TiAlN multilayer until reaching a TiN/TiAlN nano-multilayer coatings.

The addition of Al in a binary CrN coating is not always beneficial because it has a negative effect on scratch resistance.[4] Contrary to CrN coating, the addition of Al in another binary TiN showed an improvement in the mechanical capacity of coatings. However, the mechanical performance obtained is directly related to the deposition conditions, coating compositions, and also coating structures. In reality, the link between the deposition conditions, microstructure, and mechanical

properties of thin films is currently an area of intense research activity.[5] However, it is not at all clear whether the superposition of several layers in a nanoscale thin-film control to produce super-hard coatings will necessarily lead to improved mechanical behavior and adhesion performance under highly loaded contact. The aim of this work is to study the influence of the coating composition and structure on coating behavior under the two types of loading, which are the most frequently found in practice: monotone loading: the microindentation test and dynamic loading: scratch test. Therefore, damage mechanisms and different failure modes that occurred as a result of microindentation and scratch tests were discussed. These two types of tests were chosen because microindentation tests are enough to determine, at the same time, hardness[6] and adhesion coating. Then, scratching is the well-known adhesion test.[7]

Experimental details

Substrate material and coatings deposition

The substrate used in this study was 100C6 steel (AISI 52100) (1.35% Cr, 0.95% C, 0.15% Si, 0.25% Mn, 0.03% P, 0.025% S, 0.1% Mo, and Fe balance) with 22-mm diameter and 5-mm thickness. The samples were polished with 1-μm-diamond powder corresponding to a surface roughness (Ra) of approximately 0.1 μm and were ultrasonically cleaned with acetone and ethanol in an ultrasonic bath for 10 min before being dried and placed into the PVD deposition chamber. All coatings were deposited in a commercial PVD magnetron sputter-unit from Balzers (France). The targets were either pure titanium or aluminum from which titanium and aluminum plasmas were generated, respectively. The deposition was conducted in an Ar and N_2 atmosphere. During the deposition, Ar pressure was initially set and N_2 as the reactive gas was subsequently added to obtain the desired gas composition by maintaining a total working pressure constant of 1.33×10^{-4} Pa. The distance between the cathode and the substrate was kept constant at 10 cm and with a substrate temperature of 400°C. Under these conditions, TiN/TiAlN coatings were deposited at rotation speeds of the substrate turntable of 2.5 revolutions min^{-1} using a two Al and Ti stoichiometric targets with purity of 99.9%, and with an r.f. source (13 MHz). TiN/TiAlN nano-multilayer coating had a multilayered nanostructure with alternating TiN and TiAlN layers. Each individual layer had an even, uniform thickness; however, different layers had different thicknesses. The TiN and TiAlN layer thicknesses did not vary from layer to layer. The individual layer thickness (TiN or TiAlN) was controlled by the switch time of alternate shutters which were modulated by a programmable logic control. The bilayer number (n) was about 50, which gave a bilayer period (λ) of about 84 nm. The total

thickness of the coating was maintained at about 4.2 μm. In addition, a titanium (Ti) interlayer between the 100C6 steel substrate and the top layers was deposited to improve the coating adhesion.

The schematic illustration of TiN/TiAlN nano-multilayer is shown in Fig. 1.

The structure, the thickness of each layer, the number of layer of each coating, and the total thickness of the coatings are summarized in Table 1.

Characterization tests

The morphological and microstructural characterizations were evaluated by using atomic force microscopy (AFM) and scanning electron microscopy (SEM). Coating residual stresses were determined by XRD using the $\sin2\psi$ method, and the experiments were carried out with the portative diffractometer DRP-3, based on the $\sin2\psi$ method. During stress measurements, the specimen was irradiated with high-energy X-rays penetrating the surface and diffracting according to Bragg's law: $2d\sin\theta = n\lambda$, where n is the order of interference, λ is the wavelength of the X-ray, d is interplanar spacing, and θ is the angle of incidence of the X-ray beam. Vickers microindentation tests were performed with a Shimadzu HMV-2000 hardness testing machine that yielded hardness measurements with loads of 1–5 N during a holding time of 15 s. After the discharge, the imprint that was left on the surface was analyzed by SEM. This method provided an assessment of the mechanisms of cracking created during the indentation. Scratch test was performed with a scratch-tester (CSM Instruments, Switzerland) which was equipped with Rockwell HRC penetrator with the tip of 120° cone angle and 100-μm radius. The loading speed was 50 N/min, and the track length was 3 mm. The normal force of the indenter onto the coatings surface increased continuously from 3 to 30 N.
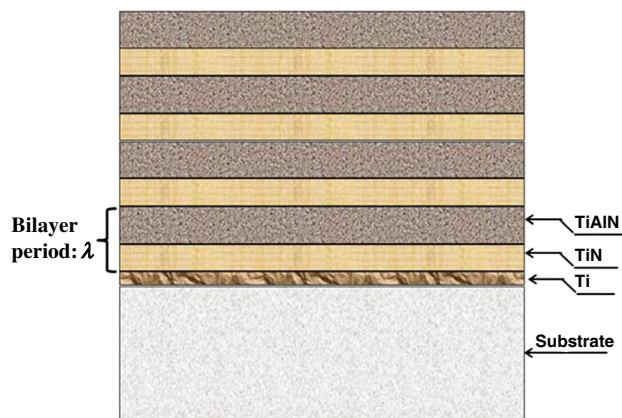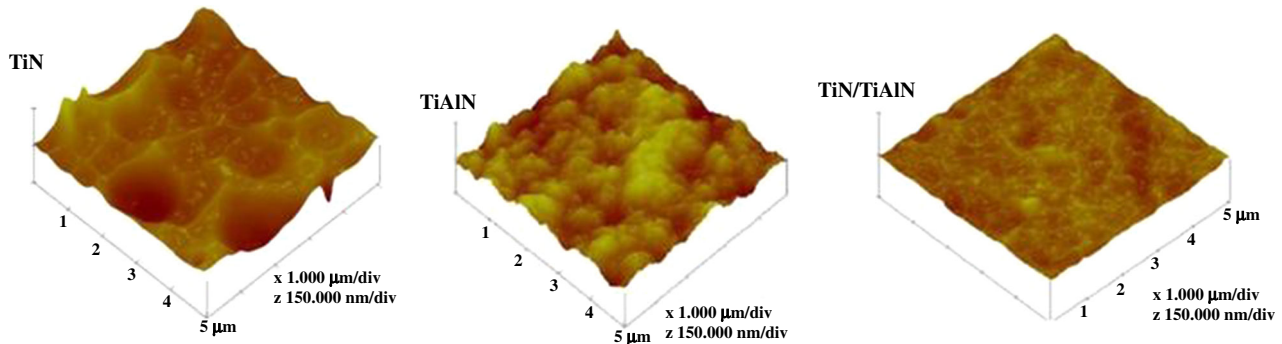

Fig. 1: Schematic illustration of TiN/TiAlN nano-multilayer

Table 1: Coating structures and thicknesses

Coatings	Number of layer	Structure		Thickness (nm)	Total thickness (nm)
TiN single layer	2	Ti/TiN	Ti	100	1000
			TiN	900	
TiAlN multilayer	3	Ti/TiN/TiAlN	Ti	100	3000
			TiN	400	
			TiAlN	2500	
TiN/TiAlN nano-multilayer	100	Ti/[TiN/TiAlN]n n = 50	Ti	100	4200
			TiN	48	
			TiAlN	36	

Fig. 2: Three-dimensional AFM images of TiN single layer, TiAlN multilayer, and TiN/TiAlN nanolayer

Results and discussion

Morphological and structural properties

Results obtained by AFM observation are illustrated in Fig. 2.

The AFM examination revealed the presence of domes and craters which were uniformly distributed over the surface. However, we noticed a difference in the size of the domes and craters that characterized the morphology, as is shown in Fig. 3.

The value of the average surface roughness was calculated as the deviations in height from the profile mean value. Results are illustrated in Table 2. TiN/TiAlN nano-multilayer structured film has a less rough surface. This was explained by the small grain size because the phase distribution is nanoscale in this coating. Indeed, AFM results of TiAlN film indicated that the increase in the number of layers in order to have a nano-multilayer structure resulted in a decrease in both the grain size and surface roughness due to nucleation matters.

SEM cross section of all coatings showed a columnar structure as shown in Fig. 4 that is similar to that proposed by Thornton[8] in his model of thin-film growth.

Residual stresses

The results of residual stress measurements are illustrated in Table 2. This indicates that the values of residual stresses vary from one coating to another. However, all coatings were characterized by compressive stress type.

The multilayer structure offered the highest residual stresses. This phenomenon is related to the coating thickness and the distribution of layers. Indeed, for the same thickness, the compressive residual stress was increased when the coating consisted of several layers. In addition, the difference between the modulus of elasticity 320 GPa for TiN and 360 GPa for TiAlN (results obtained by nanoindentation test) of layers and the others, added to interfacial interactions, and accentuated the intensity of residual stresses. In a multilayer system, the hardness enhancement mechanism is usually explained by the difference in the elastic modulus or existence of coherent interface. The former is related to Koehler theory,[9] which attributed the hardness anomalies to the modulus difference. The latter, however, deduced the Gahn's coherent strain model,[10] which suggested that it exists a coherent stress–strain field in the multilayer's films. In the present study, there is little difference in elastic modulus between the constituent materials of TiN and TiAlN. However, the presence of stress in the interface is possible.

Microhardness measurements

Vickers pyramid indentations were made with a testing machine that allows the hardness measurements at loads in the range of 1–5 N. This unit was equipped
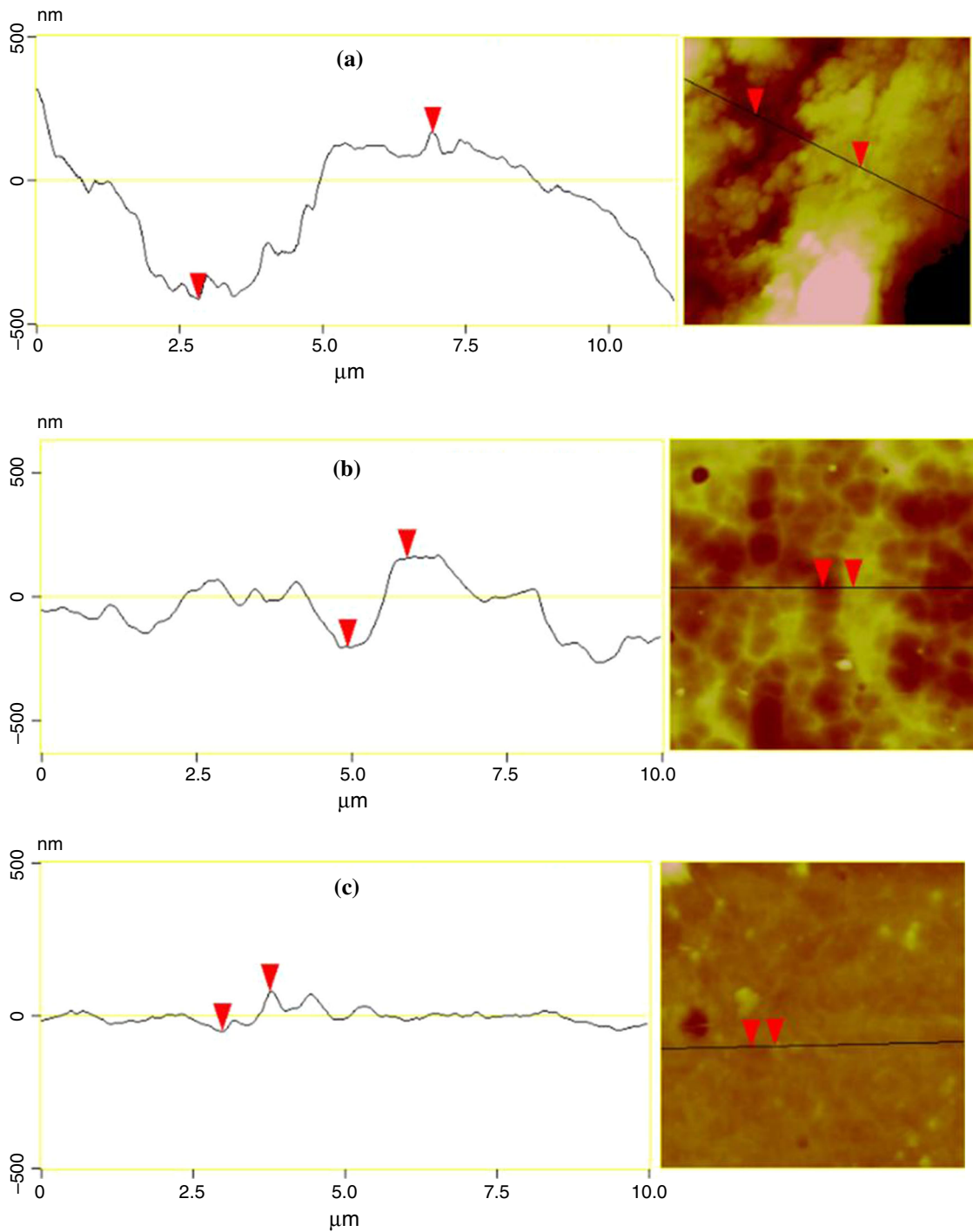
Fig. 3: Roughness profiles and 2D AFM images of (a) TiN single layer, (b) TiAlN multilayer, and (c) TiN/TiAlN nano-multilayer

Table 2: Residual stress and hardness of coatings

Coatings	Residual stresses (GPa)	Hardness (GPa)	Roughness (nm)
TiN single layer	−2.5	18	27
TiAlN multilayer	−3.5	26	20
TiN/TiAlN nano-multilayer	−4	35	11

with an optical system facilitating the measurements of the indentation diagonal.

Nevertheless, hardness measurements on materials with thin surface layers are influenced by the mechanical properties of both the substrate material and the coating. There exist three regions of hardness, namely, film only hardness H_f, composite hardness response of both film and substrate H_c, and finally substrate only hardness H_s.[11] The composite hardness H_c was calculated from the experimentally measured indentation diagonal according to the conventional Vickers method. Results of hardness measurements of the substrate coating system of the three coatings are given in Fig. 5.

After plotting the results on a graph, a linear regression showing hardness decreases as a function of applied load because of a substrate influence. The general principles of microhardness measurements must, in the case of thin layers, additionally take into account the effect of the substrate. In 1965, Buckle[12] proposed that the hardness of a material with a coating

H_c could be expressed as the sum of the weighted hardnesses of the coating H_f and the substrate H_s

$$H_c = aH_f + bH_s, \qquad (1)$$

where a and b are coefficients-influence, respectively, of film and substrate and $a + b = 1$.

Several other propositions were later developed (ref) in modeling hardness measurements of the coated systems. In this work, we used the Jonsson and Hogmark model.[13] Jonsson and Hogmark (J–H) proposed a model based on the area law of mixtures. By using simple geometrical considerations, they have separated the substrate and the film contributions.

$$H_c = \left(\frac{A_f}{A}\right)H_f + \left(\frac{A_s}{A}\right)H_s, \qquad (2)$$

where A_f is the area on which the mean pressure H_f acts, A_s is the area on which the mean pressure H_s acts, and A is the total projected area deformed. The area ratios are given by

$$\left(\frac{A_f}{A}\right) = 2C\frac{t}{h} - C^2\frac{t^2}{h^2} \text{ and } \left(\frac{A_s}{A}\right) = 1 - \left(\frac{A_f}{A}\right) \qquad (3)$$

where t is the thickness of the film, h is the indentation depth, and C is the $\sin 2\varphi = 0.136$ for soft films and $C = 2 \sin 2(\varphi/2) = 0.07$ for hard and brittle films; $\varphi = 21.6°$ for Berkovich indenter[14]; and $H_s = 9$ GPa.

Microhardnesses of the TiN single layer, TiAlN multilayer, and TiN/TiAlN nanolayer coatings as a function of applied load are shown in Fig. 6.

It can be observed that microhardness evolutions are the same for all compositions. The films hardnesses of TiN single layer, TiAlN multilayer, and TiN/TiAlN nano-multilayer, respectively, are obtained using this model and are illustrated in Table 2. The improvement of microhardness when we pass from TiN to TiAlN is linked to two sources. The addition of Al in a binary TiN coating improves the coatings hardness. First, because of its intrinsic properties, Al has a smaller grain size compared to Ti; therefore, the inter-atomic
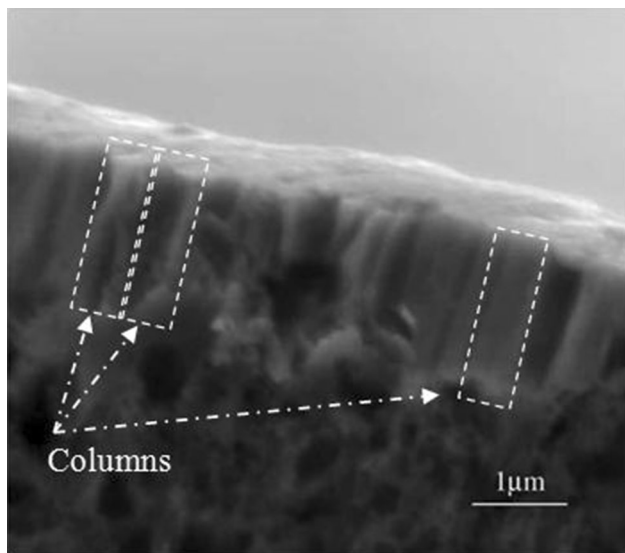
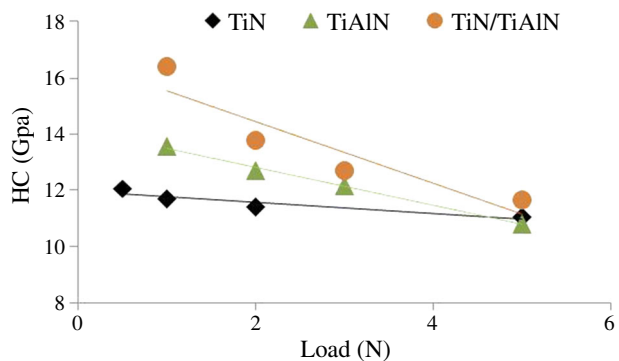

Fig. 4: Cross section SEM micrographs of TiAlN coatings

Fig. 5: Regression of hardness measurements of the composite (substrate + coating) system
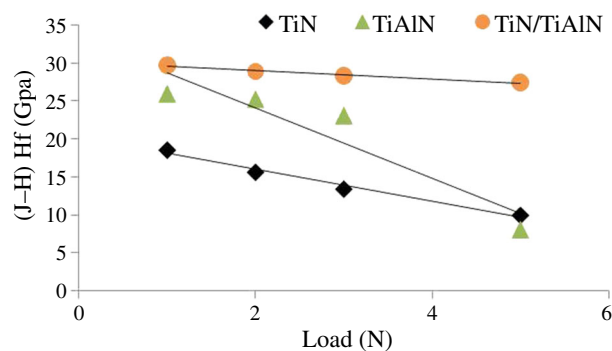

Fig. 6: Variation of H_f as a function of applied load for TiN, TiAlN, and TiN/TiAlN coatings

distance decreases, which enhances the covalent energy giving a more compact film. Second, by the addition of Al, we obtained a multilayer structure (Table 1). This is further proven with the results of the hardness of the nano-multilayer. It is for this reason that the highest microhardness value was found in the nano-multilayer structure. To sum up, the evaluated microhardness of the TiN/TiAlN nano-multilayer coating (35 GPa) was found to be considerably higher than the TiAlN multilayer coating (26 GPa) and single-layer coating (18 GPa). The hardening of this nano-multilayer structure was attributed to the following: On one hand, hardening can be explained by the Hall–Petch effect[15] because of the grain size refinement discussed in the previous paragraph (Figs. 2 and 3). On the other hand, the presence of the nanolayered structure of TiN/TiAlN coating can increase the hardness based on the widely accepted concept of blocking of dislocation motion at the layer interfaces. This is due to differences in the shear modules of the individual layer materials, and by coherency strain causing periodical strain–stress fields in the case of lattice-mismatched multilayer films.[16]

Micromechanisms of coating damage

Vickers indentation can produce various responses in coatings. These are connected, inter alia, with the elastic and plastic behavior of the substrate and coating (without cracking), cracking of the layer directly beneath the indenter, or cracking and penetration of the indenter into the substrate, combined with elastic deflection of the coating.[17] Indentations in the steel specimens with different variants of coatings were examined with an SEM. Representative images are presented in Figs. 7 and 8 which illustrate characteristic types of damage.

The increase of the applied load caused an increase in the imprint size and cracking mechanisms for all coatings. However, what was noted was the difference in damage mode occurring in each coating (Fig. 8).

According to Richter et al.,[17] cracking mechanisms can be divided into four categories: Radial cracks along extensions of the indentation diagonals (type I), outer circumferential cracks together with cracking along the indentation edge (type II), inner circumferential cracks (type III), and radial cracks which are not extensions of the indentation diagonal [so called "claws"-(type IV)].

To facilitate the analysis of a large number of results (three coatings, three types of structures, four types of cracks, and variable load), we recorded in Table 3 the cracking mechanism, after an indentation test with variable load for each coating. We marked the presence of each type of crack by a plus sign (+) and its absence by a minus sign (−).

For the lowest load 1 N, cracks are initiated at TiN single layer, while the TiAlN multilayer and TiN/TiAlN nano-multilayer have only plastic deformation. Delay of appearance of the cracking phenomenon in

these two coatings is explained by better adhesion in multilayer structures. As we explained in our previous studies of CrN and CrAlN coatings deposited on the same substrate 100C6 steel,[4] only type II crack and type III crack were observed for the TiN single layer and TiN/TiAlN nanolayer. TiAlN multilayer showed exception by the presence of a type I crack and type IV crack. Indentation method, because of its simplicity, is widely used for both qualitative and quantitative evaluation of coatings. That is why a quantitative analysis of cracks provided a thorough exploitation of the results as shown in Fig. 9.

The increase in the applied load leads to an increase in the cracking mechanisms and crack length of all coatings. In our study, film of a single layer or more, the behavior of composite (film/substrate) does not show a major difference because we are still in the coatings with low ductility. Nevertheless, the crack length is not the same in the whole coatings. It appears that the failure mode under a Vickers indentation depended on the coating composition and structure because these two parameters have a significant effect on the crack propagation. For all types of existing cracks, the passage from TiN single layer to TiAlN multilayer or TiN/TiAlN nanolayer provides a decrease in crack length. Type II crack, the type that exists in whole coatings, decreases from 177 μm for TiN single layer to 67 μm for TiAlN and 22 μm for TiN/TiAlN nanolayer. This decrease has been explained by the increase of the number of layers. Thereafter, increasing the number of interfaces that are barriers limits crack propagation and delays the film damage.

Cracks in the TiN/TiAlN coating, even if they exist, can be stopped at each interface and can cause a delamination of the top layer. This nanolayer architecture improved coatings adhesion. This agrees with the literature.[18] This result does not hold if we move from the CrN single layer to CrAlN multilayer.[4] The appearance of type I and type IV cracks in the TiAlN multilayer coating is probably related to several parameters: a high concentration of tensile stress with the imprint diagonal, an incompatibility of deformation between the substrate and the TiAlN coatings, the major difference between the film hardness and substrate hardness (26 GPa for TiAlN and 11 GPa for the substrate), and also the difference in coefficient of thermal expansion (7.5×10^{-6} K^{-1} and for the TiAlN and 11.4×10^{-6} K^{-1} for the 100Cr6). This difference is less important in the case of TiN (9.4×10^{-6} K^{-1}).

Analysis of damage mechanism by scratch test

Scratch methodology was used to evaluate the relative adhesive and cohesive failure.[19] Progression of scratching is accompanied by successive degradation described by cohesive failure signaled by microcracks at the edge, local chipping of the coating from its
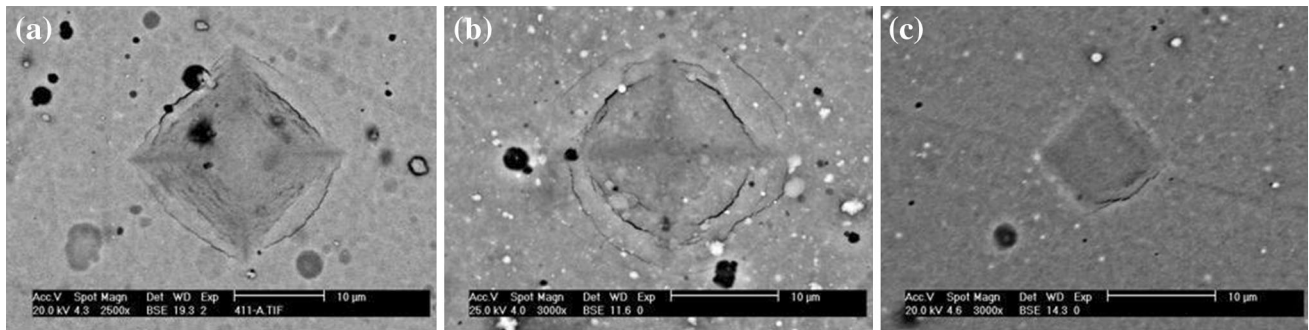
Fig. 7: Micrographs of microindentation imprints of TiN single layer (a), TiAlN multilayer (b), and TiN/TiAlN nanolayer (c) under loads of 2 N
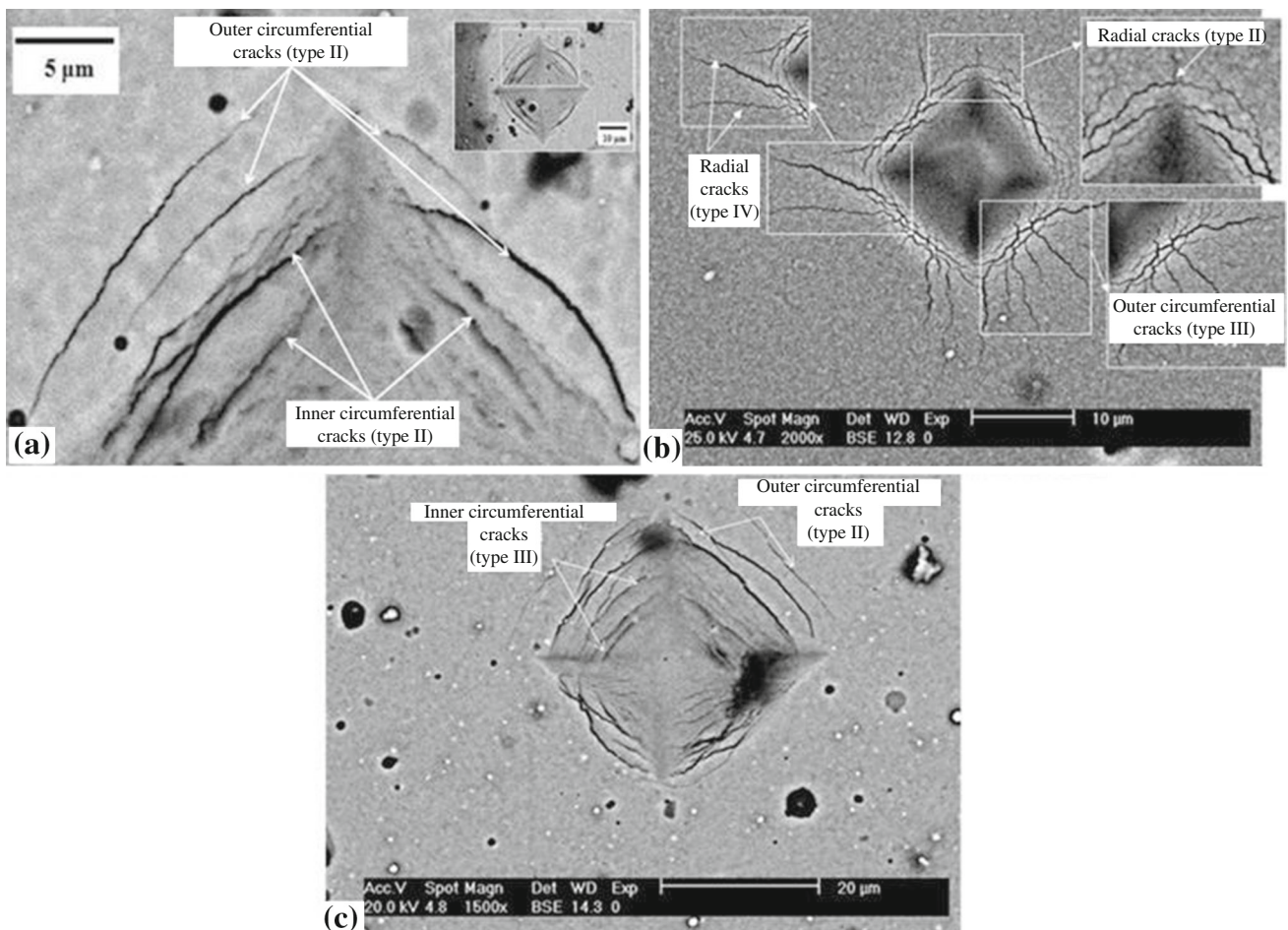

Fig. 8: Micrographs of microindentation imprint of TiN single layer (a), TiN multilayer (b), and TiN/TiAlN nano-multilayer coatings (c)

substrate, and finally, a total loss of adhesion between the two constituents as shown in the TiN single layer (Fig. 10).

Figures 11, 12, and 13 show the tracks corresponding to the TiAlN multilayer and TiN/TiAlN nano-multilayer coating after the scratch test.

Under the same loading conditions, the coating's behavior is different. In the single-layer structure, with the increase of the scratch load, cracks have been developed throughout the cross section of the film and have spread rapidly. In this type of coating, adhesive failure occurred for low load comparing to the other coatings and we observed a total chipping of the film and exposure of substrate at higher load.

In this single-layer structure, the crack was initiated along the scratch channel at a certain load, and was

Table 3: Qualitative observation of cracks types under a Vickers indentation

Coatings/load	1 (N)				2 (N)				5 (N)		
	(I)	(II)	(III)	(IV)	(I)	(II)	(III)	(IV)	(II)	(III)	(IV)
TiN single layer	–	+	+	–	–	+	+	–	+	+	–
TiAlN multilayer	–	–	–	–	+	+	–	+	+	–	+
TiN/TiAlN nanolayer	–	–	–	–	–	+	–	–	+	+	–
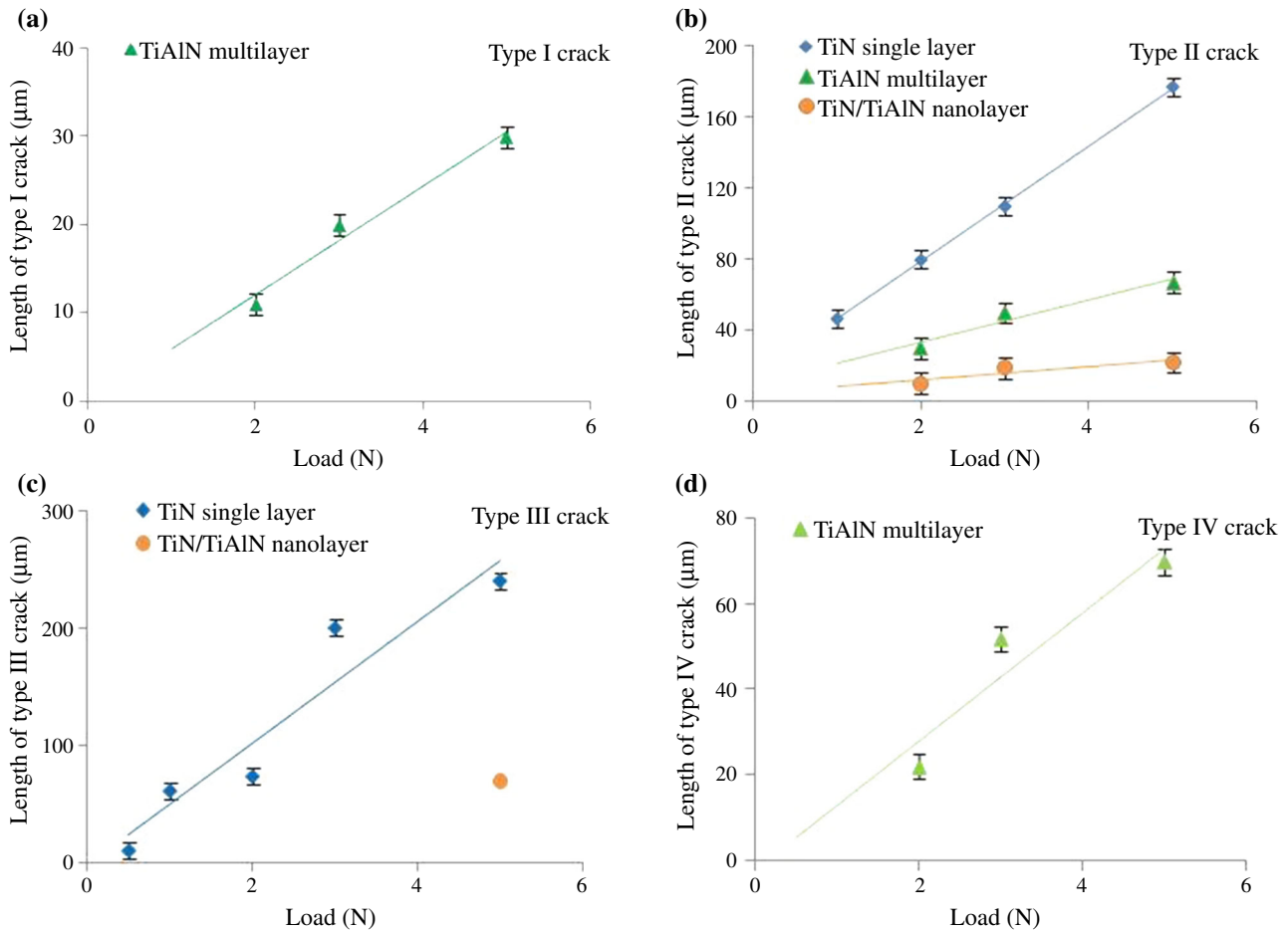
Fig. 9: Variation in type I (a), type II (b), type III (c), and type IV (d) crack length with applied load

followed by a complete delamination leading to the failure of the coating.

In the TiAlN multilayer structure, however, adhesive failure was observed at the end of the scratch track for the highest loads. Contrary to chromium-based coating,[4] the addition of Al in a binary TiN coating improves the adhesion and resistance to scratching. TiN/TiAlN nano-multilayer coating displayed small cohesive failures at the rim of the crack as shown in Fig. 13, and even for the highest loads, they showed only a small semicircular cracks (Fig. 13). This is probably due to a brittle behavior because of the high hardness (35 GPa) of this coating and the high compressive residual stresses (−4 GPa) as illustrated in Table 2 compared with −2.5 GPa for single-layer coating. Indeed, the mobility of cracks is mainly governed by the stress field in the films. Compressive residual stresses that characterize the multilayer structure have a very important role in delaying the crack propagation, and in improving fracture resistance of

the coating. Similar results were found in the other work as shown in Fig. 14.[20]

Adhesion measurement

As for microindentation tests, qualitative analysis of scratch tracks was extended to a quantitative analysis by measuring the critical load values in order to have an idea about the coatings adhesion.

The critical load is the normal load at the first coating failure detected. This load was determined by the combination of observations of scratches by optical microscopy, measurements of acoustic emission, measurements of normal and tangential loads, and the measurements of residual depth during scratch testing.

Several authors[7] have linked the appearance of the first crack (cohesive failure) at a first critical load noted by L_{c1}, and the upper critical load at which the first delaminating at the edge of the scratch track occurred (adhesion failure) by L_{c2}. At a higher applied load at which the damage of the film exceeds 50% or a total loss of adhesion between film and substrate that indicates a full interfacial failure.

Critical loads L_{C1}, L_{C2}, and L_{C3} were investigated. The multilayer coatings showed only critical loads L_{C1} and L_{C2}, while the TiN single layer showed a total chipping of the film at a critical force L_{C3} equal to 12.3 N.

Critical loads L_{C1} and L_{C2} were investigated as a function of the coating structure (see Fig. 15).

Critical load is very influenced by the coating structure. It appeared clearly that thin film with the greater number of layers can contribute to higher critical load. TiN/TiAlN nano-multilayer thin film has the highest critical loads which mean that the adhesion on the substrate is significantly improved in the multilayer thin film compared to the single-layer thin films. In multilayer structure coatings, cracks develop mostly in the vicinity of the upper surface, and the layers interfaces can change the initial crack orientation.

We calculated the average friction coefficient after scratch test of all coatings and the values obtained are shown in Fig. 16.

Figure 16 shows that the layer which has the lowest critical load has the lowest coefficient of friction and the opposite. Therefore, the friction coefficient increases when the critical load increases.

The passage from TiN single layer to TiAlN multilayer and to TiN/TiAlN nano-multilayer coatings increases the critical load, this also increases the friction coefficient during the scratch test. The increase of friction coefficient with the increase of critical load is due to the increasing of plastic deformation resistance because of the increase of hardness and residual stresses.
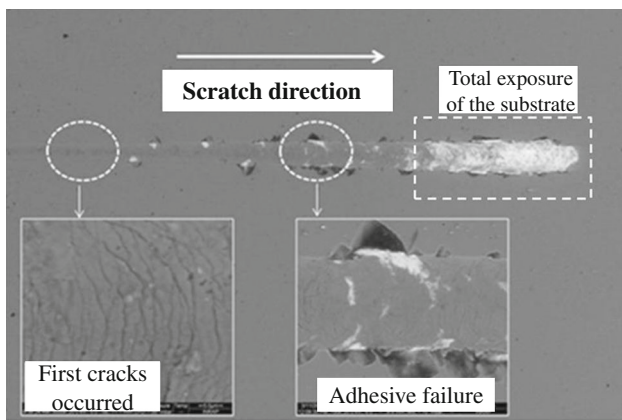

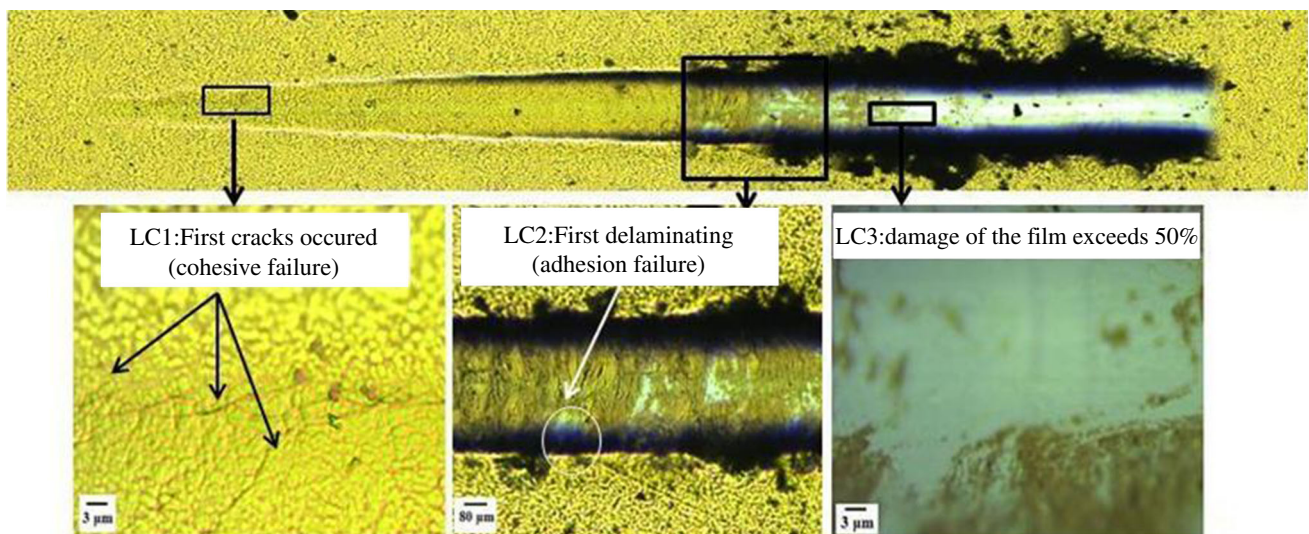Fig. 10: SEM micrographs of scratch tracks of TiN single layer

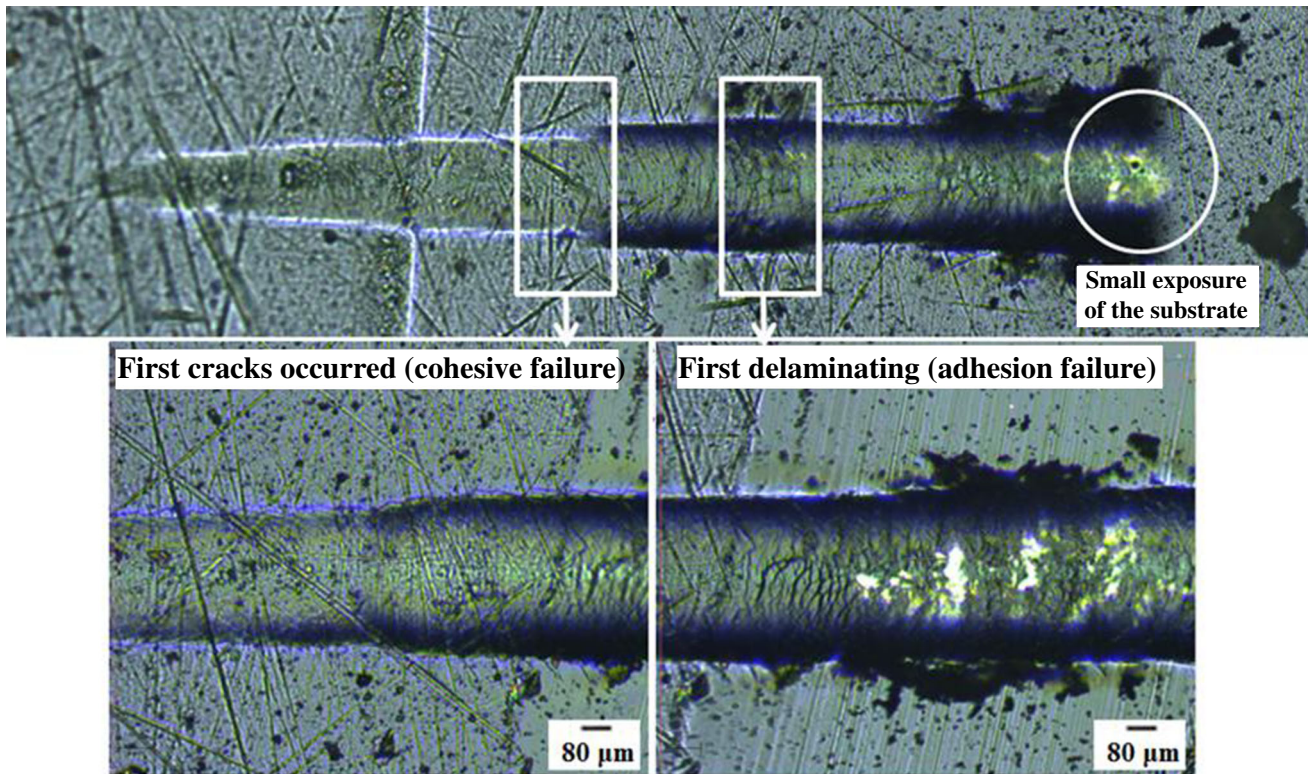Fig. 11: Optical micrographs of the scratch track of the TiN single-layer coating

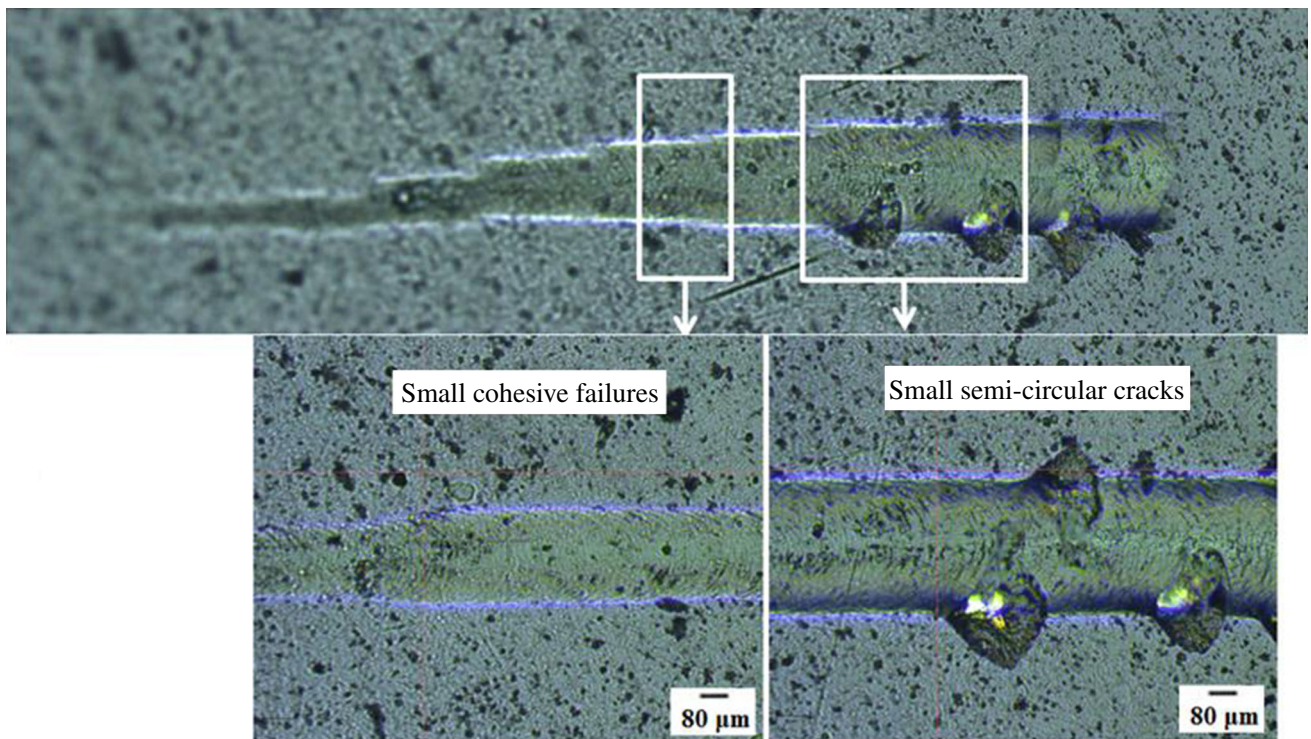**Fig. 12:** Optical micrographs of the scratch track of the TiAlN multilayer coating

Fig. 13: Optical micrographs of the scratch track of the TiN/TiAlN multilayer coating
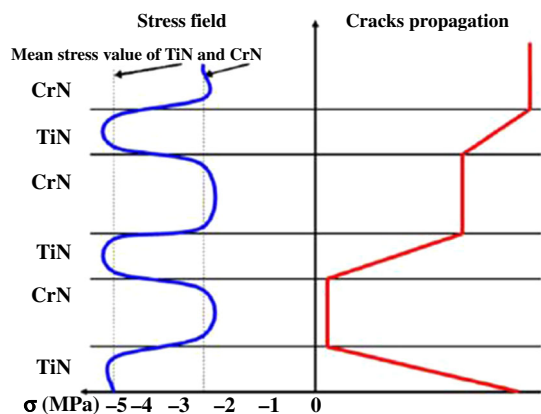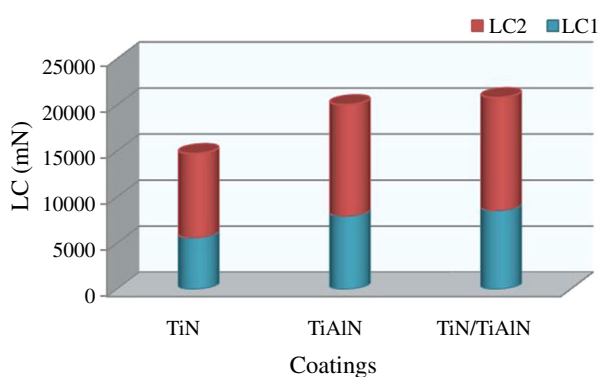
Fig. 14: Crack propagation of TiN/CrN multilayer[20]

Fig. 15: Critical loads L$_{C1}$ and L$_{C2}$ of TiN single layer, TiAlN multilayer, and TiN/TiAlN nanolayer coatings
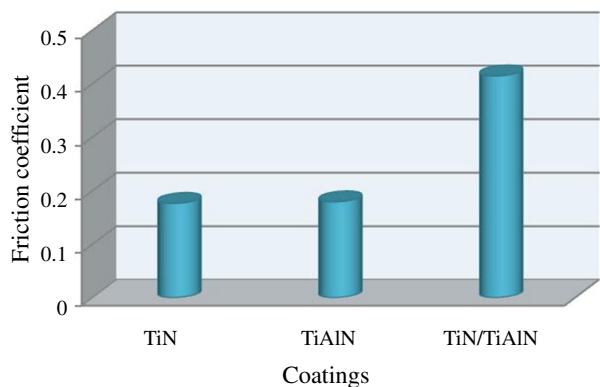

Fig. 16: Friction coefficient of TiN single layer, TiAlN multilayer, and TiN/TiAlN nanolayer coatings

Then, it is clear that mechanical properties and multilayer structure control the scratch behavior. Films with higher hardness and higher residual stresses (Table 2) show more friction coefficient and more scratch resistance. Scratch resistance may also be related to the increase in the coatings thickness and roughness (Table 2).

Conclusion

In this work, PVD thin films with different structures, single layer, and multilayer coatings, were deposited on 100C6 (AISI 52100) steel substrate by PVD magnetron sputtering system. The morphological and microstructural properties were evaluated by using atomic force microscopy (AFM) and SEM. Residual stresses were evaluated by XRD using the sin2ψ method. Hardness as a fundamental mechanical property was evaluated with microindentation test and Jonsson and Hogmark model. Adhesion quality was studied with microindentation and scratch tests. Damage's mechanisms that had occurred during testing indentation and scratch testing were further discussed. The major conclusions are the following:

- The AFM examination revealed the presence of domes and craters which are uniformly distributed over the surface. TiN/TiAlN nanostructures have a less rough surface because of the small grain size with a nanoscale phase distribution.
- The SEM cross section of all coatings showed a columnar structure.
- Compression residuals stresses were found in all coatings with a high value of -4 GPa for TiN/TiAlN nanolayer coatings.
- Application of the Jonsson and Hogmark prediction model was efficient for determining the coatings hardness and it was found film hardness of 18, 26, and 35 GPa of TiN single layer, TiAlN multilayer, and TiN/TiAlN nano-multilayer, respectively. The highest microhardness was measured for the nanolayer coatings.
- Damage mechanisms under microindentation and scratch depended on coatings structure and composition. Only type II cracks and type III cracks were observed for the TiN single layer and TiN/TiAlN nanolayer.
- TiAlN multilayer showed exception by the presence of type I crack and type IV crack. The addition of Al in a binary TiN coating improves the coating hardness, the residual stresses, the adhesion quality, and the resistance to scratching and indentation.
- Nano-multilayer structure provides an increase of hardness, residual stress, failure resistance, and a decrease in cracks propagation because of the high number of interface. In fact, in this type of structure, the number of interfaces presents barriers that limit crack propagation and delay the film damage.
- Mechanical properties and multilayer structure of the film control the scratch behavior.

References

1. Taha, Mohamed A, El-Mahallawy, Nahed A, Hammouda, Rawia M, Nassef, Sherif I, "PVD Coating of Mg–AZ31 by Thin Layer of Al and Al–Si." *J. Coat. Technol. Res.*, **6** 793–800 (2010)

2. AL-Bukhaiti, MA, Al-hatab, KA, Tillmann, W, Hoffmann, F, Sprute, T, "Tribological and Mechanical Properties of Ti/TiAlN/TiAlCN Nanoscale Multilayer PVD Coatings Deposited on AISI H11 Hot Work Tool Steel." *Applied Surface Science*, **318** 180–190 (2014)

3. Tian, Bin, Yue, Wen, Zhiqiang, Fu, Yanhong, Gu, Wang, Chengbiao, Liu, Jiajun, "Microstructure and Tribological Properties of W-Implanted PVD TiN Coatings on 316L Stainless Steel." *Vacuum*, **99** 68–75 (2014)

4. Khlifi, K, Ben Cheikh Larbi, A, "Investigation of the Adhesion of PVD Coatings Using Various Approaches." *Surf. Eng.*, **29** (7) 555–560 (2013)

5. Pemmasani, SP, Valleti, K, Gundakaram, RC, Rajulapati, KV, Mantripragada, R, Koppoju, S, Joshi, SV, "Effect of Microstructure and Phase Constitution on Mechanical Properties of Ti$_{1-x}$Al$_x$N Coatings." *Appl. Surf. Sci.*, **1** 936–946 (2014)

6. Henry, P, Pac, M-J, Rousselot, C, Tuilier, M-H, "Wear Mechanisms of Titanium and Aluminium Nitride Coatings: A Microtribological Approach." *Surf. Coat. Technol.*, **223** 79–86 (2013)

7. Beake, BD, Vishnyakov, VM, Harris, AJ, "Relationship Between Mechanical Properties of Thin Nitride-Based Films and Their Behavior in Nano-scratch Tests." *Tribol. Int.*, **44** 468–475 (2011)

8. Škorić, Branko, Kakaš, Damir, Bibic, Natasa, Rakita, Milan, "Microstructures of TiN Films Grown by Various Physical Vapour Deposition Techniques." *Surf. Sci.*, **566** 40–44 (2004)

9. Koehler, JS, "Attempt to Design a Strong Solid." *Phys. Rev. B*, **2** 547 (1970)

10. Gahn, JW, "Hardening by Spinodal Decomposition." *Acta Metall.*, **11** 1275–1282 (1963)

11. Rupa, PKP, Chakraborti, PC, Mishra, SK, "Mechanical and Deformation Behaviour of Titanium Diboride Thin Films Deposited by Magnetron Sputtering." *Thin Solid Films*, **517** 2912–2919 (2009)

12. Buckle, H, "Les possibilités et les limites d'application des essays de microdureté pour les revêtements métalliques." *La Machine Outil Française*, **206** 125 (1965)

13. Jonsson, B, Hogmark, S, "Hardness Measurements of Thin Films." *Thin Solid Films*, **114** 257 (1984)

14. Chu, X, Barnett, SA, "Model of Superlattice Yield Stress and Hardness Enhancements." *J. Appl. Phys.*, **77** (9) 4403 (1995)

15. Santana, AE, Karimi, A, Derflinger, VH, Schutze, A, "Microstructure and Mechanical Behavior of TiAlCrN Multilayer Thin Films." *Surf. Coat. Technol.*, **177–178** 334 (2004)

16. Madan, A, Wang, YY, Barnett, SA, Engström, C, Ljungcrantz, H, Hultman, L, Grimsditch, M, "Enhanced Mechanical Hardness in Epitaxial Non-Isostructural Mo/NbN and W/NbN Superlattices." *J. Appl. Phys.*, **84** 776 (1998)

17. Richter, J, "Application of Vickers Indentation for Assessment of PVD TiN Coated New Nonledeburitic High-Speed Steels." *Surf. Coat. Technol.*, **162** 119–130 (2003)

18. Lee, H-N, Raghavanpillai, A, Li, J, Pollino, JM, Rosen, BM, Shenoy, SR, "Comparative Examination of Adhesive and Cohesive Properties of Fluorinated Coatings on Stone/Tile Surfaces." *J. Coat. Technol. Res.*, **11** 933–942 (2014)

19. Ipaz, L, Caicedo, JC, Esteve, J, Espinoza-Beltran, FJ, Zambrano, G, "Improvement of Mechanical and Tribological Properties in Steel Surfaces by Using Titanium–Aluminum/Titanium–Aluminum Nitride Multilayered System." *Appl. Surf. Sci*, **258** 3805–3814 (2012)

20. Mendibide, C, Steyer, P, Fontaine, J, Goudeau, P, "Improvement of the Tribological Behaviour of PVD Nanostratified TiN/CrN Coatings—An Explanation." *Surf. Coat. Technol.*, **201** 4119–4124 (2006)